RSC Advances

Enhanced dielectric and ferroelectric properties in NaTNO/PVDF nanocomposites: A new flexible material for capacitor application

Journal:	*RSC Advances*
Manuscript ID:	RA-ART-03-2015-003883.R1
Article Type:	Paper
Date Submitted by the Author:	08-Apr-2015
Complete List of Authors:	Bhadra, Debabrata; Bhairab Ganguly College, Department of Physics Sarkar, S; Jadavpur University, Center for Rural and Cryogenic Technology Chaudhuri, Bijay; NIT Rourkela, Department of Physics

Enhanced dielectric and ferroelectric properties in NaTNO/PVDF nanocomposites: A new flexible material for capacitor application

D. Bhadra[a], S. C. Sarkar[b] and B. K. Chaudhuri[b,c]*
[a] Department of Physics, Bhairab Ganguly College, Belgharia, Kolkata-700056, India
[b] Center for Rural and Cryogenic Technology, Jadavpur University, Kolkata-700032,India
[c] Department of Physics, NIT Rourkela, Orissa-769008, India

ABSTRACT: Polymer nanocomposites (*PNC*) showing improved physical properties are emerging as novel functional materials because of their adaptable physical properties for technological applications. We synthesized a new *PNC* system composed of insulating ferroelectric poly-vinylidene fluoride (*PVDF*) host and a high dielectric semiconducting $Na_xTi_yNi_{1-x-y}O$ (Na and Ti co-doped NiO with x=0.05, 0.15 and y=0.02) oxide of variable particle sizes (~0.5-0.6 μm to ~80-90 nm) as fillers. The *PNC* system exhibited excellent ferroelectric behavior as well as tensile strength with low percolation threshold (f_c). The observed large enhancement of room temperature effective dielectric permittivity (ε_{eff} ~600-750 about 60-75 times that of host *PVDF* matrix) along with very low dielectric loss of ≤0.18 at 1kHz, high dielectric breakdown voltage (>140kV/mm) and saturation polarization (~10μC/cm^2) near f_c distinguished these *PNC* films as suitable candidates for capacitor applications in devices.

Keywords: Polymer nanocomposite, percolation threshold, filler, dielectric constant, breakdown voltage.

*Corresponding author. Tel.: +916612462734.
E-mail address: sspbkc23@gmail.com

1. Introduction

Novel low loss high dielectric and high conducting polymer–ceramic composites possessing ferroelectric, piezoelectric, electro-optic or superconducting properties are always in great demand as they form a new class of functional materials for technological applications [1-2]. Moreover, many of these composites showed process compatibility, flexibility, elasticity, low density and high breakdown strength [3]. Recently ferroelectric ceramic/polymer (C/P) composites with high-ε have drawn global attention and it has also become an area of active research and development [4-6] as these composites exhibiting high dielectric constant (ε) and suitable mechanical properties could be prepared at ambient or moderate temperature and could also be fabricated as per specific requirements by tailoring the relative concentrations and modulation of surface property of the fillers [7]. However, as polymeric materials, in general, suffer from very low ε values (~3-10), several attempts had so far been made to enhance ε by dispersing highly conductive particles in the polymer matrix [7-8] showing increase of dielectric constant but with higher dielectric loss and degradation of physico-mechanical properties. Interestingly, composites showing high dielectric/conducting properties at lower percolating thresholds may maintain the desired flexibility and mechanical strength and, therefore, highly important for technological applications. The enhanced effective dielectric constant (ε_{eff}) and AC conductivity (σ_{eff}) of the polymer composites near the percolation threshold could be understood applying the concept of the aforesaid percolation theory [9]. The percolation threshold value might, however, change significantly depending on the shape, surface morphology and size of the fillers and their processing conditions [10-12]. Dramatic increase of ε_{eff} close to the percolation threshold, as observed in some conductor-insulator percolative system, stimulated interest for the development of semiconductor-polymer bulk and nanocomposites as they form a novel group of materials for capacitor applications [13-19]. Here it should be mentioned that the percolating behavior of different micro and nano scale materials as fillers might be used to create composites with enhanced physical properties, because of the changes of their surface morphologies and nano-structural features, have not been well investigated.

It is well known that piezoelectric semicrystalline polymer, polyvinylidine fluoride (PVDF) has been vastly used to enhance ε_{eff} of composites, for instance, in the $BaTiO_3$/PVDF and Li doped NiO(LNO)/PVDF systems, where ε_{eff} increased substantially (~50–400) at high filler concentrations (volume fraction>0.6). But it led to high mass density and also weak

mechanical property of the composites [20-21]. Recently, Dang *et al.* observed weak percolation effect and enhanced dielectric constant of ~49 in polyimide composite using a high dielectric bulk $CaCu_3Ti_4O_{12}$ (CCTO) as the filler.[21] Remarkable enhancement of dielectric properties in the conductor-insulator bulk composite was observed, prepared mostly by the simple melt-blending method [19–21]. However, due to its percolation nature, the electric and dielectric properties of a percolative composite are very sensitive to the composition and surface morphology of the fillers. In addition, the dielectric loss tangent (*tanδ*) of a percolative composite is usually high. The energy loss, positively related to the dielectric loss, can be determined by the equation: $W \approx \pi\varepsilon\xi^2 f \tan\delta$ (where ξ is the electric field strength and f is the frequency). As such, a low dielectric loss is preferred in order to reduce the energy loss from a dielectric material, particularly for high frequency applications. Because of the modern trend of device miniaturization, high performance and lower electric power consumption in micro-electromechanical systems (*MEMS*), high ε_{eff} materials have got enormous demand in current research and development. However, as percolative behavior depends on various factors, before the applications of any new composite material in devices, elaborate characterization and study of low percolative threshold behavior, providing the optimum concentration are utmost necessary for gaining maximum efficiency.

Recently a lead-free multicomponent perovskite ceramic materials like viz. $A_xTi_yNi_{1-x-y}O$ (A=Li, K & Na) [22, 23] had been synthesized both in their nano and microcrystalline forms exhibiting colossal dielectric constant (~10^4) in its polycrystalline form [22-24], which might be important candidates for making high-ε flexible polymer nanocomposites (PNC) for various applications. In such a system, microstructure of the filler affected the real part of dielectric permittivity and the loss tangent, for instance, in NaTNO ($Na_xTi_yNi_{1-x-y}O$; x=0.05, 0.15, y=0.02) exhibiting some distinguishing dielectric and micro-structural behavior [22-24] compared to those of other members (viz. LTNO and KTNO with Li and K monovalent cations, respectively) [25-28]. Since dielectric as well as magnetic properties of such composite materials are very much dependent on the particle size of the fillers, PVDF composites made with nano and micro NaTNO fillers might also have some distinguishing dielectric and other physical properties near the percolation thresholds [26-32].

Therefore, in the present paper we made a comparative study of the PVDF composites formed with micro and nanoparticles of the above mentioned two high dielectric systems. $Na_{0.05}Ti_{0.02}Ni_{0.93}O$ (abbreviated as *NaTNO-1*) and $Na_{0.15}Ti_{0.02}Ni_{0.83}O$ (abbreviated as *NaTNO-2*) showed real part of dielectric constant $\varepsilon'=2.5\times10^3$, 5×10^3 and $\tan\delta\approx10$, 11 at 100Hz in room temperature [30]. Different Na/Ti ratios in such materials would not only change the percolation threshold behavior [33-38] but also affect the grain/particle size, crystallinity and also dielectric as well as electrical behavior of the prepared composites. Since low percolation limit is desired for high flexibility and breakdown strength (important prerequisites for applications in devices), we mainly focused our discussion on the samples with NaTNO-1 nanoparticles (*nps*) as the suitable filler, compared to other prepared micro and nano sized fillers, due to its enhanced breakdown voltage, tensile strength and of course low percolation threshold.

2. Experimental

2.1. Materials

PVDF with average molecular weight (M_w~ 534,000) was procured from the Aldrich (USA). N, N-dimethylformamide (DMF) (Junsei chemical co., India), $Ni(NO_3)_2$,$6H_2O$ (99.9 % purity of Merck), Na_2CO_3 (Merck, 99.9%), citric acid [$C_6H_8O_7$] (Merck, 99.9%) and ([CH_3 $(CH_2)_3O]_4$ Ti) (Aldrich, 99.5%) were also used for sample preparation. Other materials like TiO_2 and Ni_2CO_3, $Ni(OH)_2$,$4H_2O$ with purity of 99% were purchased from local agents. All materials used without further purification.

2.2. Methods

The ceramic $Na_{0.05}Ti_{0.02}Ni_{0.93}O$ (NaTNO-1C) and $Na_{0.15}Ti_{0.02}Ni_{0.83}O$ (NaTNO-2C) samples were prepared by the conventional solid state synthesis using Na_2CO_3, TiO_2 and Ni_2CO_3, $Ni(OH)_2$,$4H_2O$. Stoichiometric amounts of these powders were mixed thoroughly in a mortar in presence of ethyl alcohol. The well-mixed fine powder was then baked at 873K for 24 h. The baked powder was reground and pressed into pellets of almost 1mm thickness and 4mm in diameter at a pressure of 5 tons. The final pellet was sintered again at 1273K for 30h at normal pressure. NaTNO-1C and NaTNO-2C ceramic grinded powders were thus prepared (average particle size~0.5μm). The napaparticles of $Na_{0.05}Ti_{0.02}Ni_{0.93}O$ (NaTNO-1) and $Na_{0.15}Ti_{0.02}Ni_{0.83}O$ (NaTNO-2) *nps* were prepared using simple conventional sol–gel technique. Stoichiometric

amounts of $Ni(NO_3)_2$, $6H_2O$, Na_2CO_3 and citric acid [$C_6H_8O_7$] were mixed and dissolved into an appropriate amount of distilled water. Tetra butyl titanate ([CH_3 $(CH_2)_3O]_4$ Ti) was then added slowly and the solution was heated and stirred continuously to form the gel, which was carefully dried in the oven at 120°C. The dried gel was finally calcinated at 800°C for 1 hr in air. Thus NaTNO-1 & NaTNO-2 *nps* (average particle size~80-90nm) was obtained. The preparation of the NaTNO/PVDF composite (both micro and nano with the same stoichiometry) was described as following. The PVDF powder was initially dissolved in DMF. After the solution was stirred for 8 hr at 70°C, the required amount (volume fraction) of NaTNO-1C & 2C ceramic powder as well as NaTNO-1 & 2 *nps* were poured into the PVDF host solution. The mixed solution was sonicated for about 20 min and stirred for an additional 8 hr to disperse NaTNO particles into PVDF homogenously. The final solution was poured onto a glass plate to form a cast film at 70°C in an oven for 8 hr and then hot-pressed at 200°C under 10 MPa for 15 min (pre-pressing was conducted for 5 min under the same conditions, after which the pressure was released for a while and the sample was then re-pressed for 20 min, followed by cooling to room temperature while maintaining the same pressure) to form polymer composite films. The films with different f_{NaTNO} (=0-0.25) were prepared each having 12 mm in diameter and 0.10 mm in thickness. Four types of NaTNO samples with different stoichiometric characteristics were employed in the present investigation and their physical properties were summarized in *Table I*.

2.3. Characterization

The crystalline phases of the ceramic powder, nps and composite samples were determined by X-ray powder diffraction by using Bruker AXS D8SWAX diffractometer with Cu-K_α radiation (λ=1.54 *A*°). The morphologies of the NaTNO samples were studied by a field emission scanning electron microscope (FESEM, JEOL, JSM 6700F). Microstructural properties were obtained using transmission electron microscope and high-resolution transmission electron microscope (TEM; JEOL 2010). AC electrical properties of the samples were measured using an HP 4194A impedance/gainphase analyzer in the frequency ranges of 100 Hz–13 MHz. The polished and fractured surface of the polymer composites (NaTNO/PVDF) were examined by another SEM (Carl Zeiss, EVO-MA10). The *d*33 coefficient was measured using a Take Control PM25 piezometer. The leakage current-voltage (*I-V*) characteristic with a voltage source measuring unit and the polarization-electric field (*P-E*) hysteresis loops at room temperature (*RT*) were determined by ferroelectric P-E loop tracer (Radiant Technology: PM-II). A two

terminal capacitor configuration was employed for this measurement. An Instron 5567 Universal Testing Machine (30kN capacity load cell) was used to measure the tensile modulus and strength. Based on ASTM D882-09 standard, 5 x 90 mm specimens were prepared and five tests for each sample were performed to obtain the average values. An initial gauge length of 50 mm and crosshead a speed of 10 mm/min were used according to the standard. A non-contacting advanced video extensometer (Instron) was used to measure the tensile extension of each specimen.

3. Results and Discussion

3.1. Structural and microstructural properties

Figures 1(a and b) showed the FESEM images of NaTNO-1 & 2 nanoparticles with uniform size and non-spheroid shape can be observed. As depicted in the inset of figures 1(a and b), the bulk grains which also showed uniform morphology with looser grain boundaries as those of LTNO and KTNO ceramics [22, 25-26]. The insets of figure 1(a) and 1(b) showed the TEM images of NaTNO-1 and 2 *nps*, respectively. Figure 1(c) showed the SEM micrographs of the polished surfaces of NaTNO-1 and NaTNO-2 (inset of figure 1c) polymer nanocomposites (*PNC*), having 0.08 and 0.10 volume fractions (f_{NaTNO}), respectively. The SEM micrographs of the fractured cross section and polished surface of the composite films (figures 1d and 1e, respectively) represented uniform distributions of the NaTNO-2C and NaTNO-1C ceramic particles in the PVDF matrix. With increasing f_{NaTNO}, the NaTNO particles aggregated to form large particle clusters and self-connected as a continuous percolation cluster at the percolation threshold ($f_{NaTNO\text{-}2}$=0.08=f_c) which was responsible for the divergence of dielectric permittivity as shown in the inset of figure 1(c). Figures 1 (d and f) showed the fractured cross section of NaTNO-2C/PVDF and NaTNO-2/PVDF percolative composites, where NaTNO particles were strictly separated by thin PVDF insulation layers inhibiting the formation of leakage currents at such volume fractions in the polymer composites. The *nps* retained their usual geometry in the nanocomposites after hot pressing and the grain structure had a beneficial effect in increasing the absorption properties [27]. In the percolation regime, extended networks of connected particles started to form percolative pathways that spanned across the polymer nanocomposite. As shown in figure 2(a), the X-ray diffraction (XRD) peaks of NiO could be well detected in the NaTNO-1 powders (both bulk and nano, obtained respectively, by solid state route and sol-gel techniques)

[28-29]. The samples were also found to be free from any impurity peak. Figure 2(b) presented the XRD patterns of the NaTNO-1(f_c=0.10) and NaTNO-1C (f_c=0.20) percolative composites, respectively. The XRD pattern of the hot pressed percolative composites (f_{NaTNO}=f_c) were shown, respectively, in figures 2(b) and 2(d). It was evident from these patterns that the PVDF (Figures 2 (b and d)) existed in mixed nonpolar phases of α and γ. The sharp peaks at 2θ corresponding to 17.7° (100), 18.4° (020) and 19.9° (110) were assigned to the α-PVDF. It should also be noted that the size of the crystalline domains of the PVDF host were observed to decrease with increasing *nps* volume fraction, as evidenced from the SEM images (Figures 1a and b). Such observation indicated an implication for volume fraction dependence of various (micro) nano-sized fillers on both dielectric and ferroelectric properties of the PNCs.

The effective dielectric constants depending on volume fractions of NaTNO fillers for both the NaTNO/PVDF micro and nanocomposites were shown in figure 3(a). The addition of semiconducting NaTNO both in the bulk and nano forms led to remarkable increase of dielectric constants of the composites. The dielectric constant of the sample with $f_{NaTNO-2}$=0.08 was found to be 640, which was about 64 times higher than that of pure PVDF (~ 10). Even dielectric constant of 710 was obtained for the NaTNO-1/PVDF composite with f_{NaTNO1}=0.10, which was 71 times higher than the value of pure PVDF. The dielectric property of composites with the compositions near the percolation threshold followed a scaling law. Mathematically, the effective dielectric constant of polymer composites can be described as follows: [9, 30-33]

$$\varepsilon_{eff} = \varepsilon_{PVDF}(f_c - f_{NaTNO})^{-s} \qquad \text{for} \quad f_{NaTNO} < f_c \qquad (1)$$

where s is critical exponent. From the best fitting, we got f_c= 0.10±0.01, 0.20±0.01, 0.08±0.01 and 0.18±0.01, respectively, for the NaTNO-1/PVDF, NaTNO-1C/PVDF, NaTNO-2/PVDF and NaTNO-2C/PVDF composites as shown in figure 3(b). The critical exponent s agree**d** well with the universal one ($s \approx 1$) [33]. The perceptible feature of the Na and Ti co-doped NiO composite compared to similar other systems, [9, 33-39] is the presence of more holes (or pores) in the surface morphology. This may be due to the large divergence of ionic radius mismatch of substituent atom with the parent and/or the Pilling Bedworth Ratio (called PBR).[24] Figure 3(c) showed the same trend of variation of tanδ with NaTNO content and f_c evidenced the same value as earlier. Such an increase in the loss tangent is the inevitable consequence of the significantly raised conductivity of the composite and also an important feature of percolative composites.

Figure 3(d) demonstrated the real part of the dielectric constant and AC conductivity for various Na contents of NaTNO ceramics at RT. It is clear from this figure that as Na content (0.05 and 0.15) increased the real part of ε′ and also increased loss due to larger dc-conduction [24-30]. It is also perceptible that low frequency loss is quite high which is ascribed to the inhomogeneous microstructure consisting of semiconducting grain separated by a more resistive grain boundary. It is clearly seen from the SEM images (inset of figure 3d) that ceramics with many pores and hillock morphology lead to a lower frequency dependent ε′ value.[24] It is also important to note that the Na-doped ceramics showed largest frequency dependent behavior and with the increase of Na content such frequency dependency moved to lower frequency side.[30] Figure 3(e) showed the variation of dielectric constant as a function of frequency for the pristine PVDF film along with various NaTNO/PVDF composites with different percolative volume fractions. The frequency dependence of the dielectric constant gained gradual strength as the content of NaTNO was increased. It may be argued that the large enhancement of dielectric constant of the NaTNO/PVDF composites could be attributed to the formation of the multi-layered structure. The variation of dielectric constant versus f_{NaTNO} was explained in the light of a microcapacitor model where a pair of neighboring NaTNO nanoparticles was regarded as a microcapacitor, with the NaTNO as the two electrodes and a very thin PVDF layer in between as dielectric. A network of these micro-capacitors expands between two virtual electrodes with increasing NaTNO content. Each microcapacitor contributes an abnormally large capacitance. The semiconducting NaTNO nanoparticles are considered to be close enough proximity to create pathway for charge carrier transport.

In inorganic oxide–organic polymer composites, the critical volume fraction at the percolation threshold (f_c) is a key parameter when studying their electrical properties. [9, 33-38] Near the percolation threshold, the electrical conductivity of the composite also increases by several orders of magnitude, similarly to the dielectric constant. Figure 4(a) showed the AC conductivity of the NaTNO/PVDF composites as a function of NaTNO volume fraction (f_{NaTNO}). The conductivity can further be analyzed with the critical content f_c by the power laws [33-38]

$$\sigma_{eff} = \sigma_{NTNO}(f_{NaTNO} - f_c)^t \qquad \text{for} \quad f_{NaTNO} < f_c \qquad (2a)$$

$$\sigma_{eff} = \sigma_{PVDF}(f_c - f_{NaTNO})^{-s'} \qquad \text{for} \quad f_{NaTNO} > f_c \qquad (2b)$$

where f_{NaTNO} is the filling factor, namely the volume fraction of NaTNO fillers, f_c is the percolation threshold and σ_{NaTNO}, σ_{PVDF} are the respective conductivities of the semiconducting NaTNO fillers and pure PVDF at room temperature (*RT*). In addition, t is the critical exponent in the conducting region; s', the critical exponents in the insulating region. It can be seen from figure 4 (a) that the conductivity of the NaTNO/PVDF composites clearly displays the typical insulator–conductor transition at f_{NaTNO}~0.10, 0.20, 0.08, and 0.18, respectively, for the NaTNO-1/PVDF, NaTNO-1C/PVDF, NaTNO-2/PVDF and NaTNO-2C/PVDF composites. The best fitting of the conductivity data to the log-log plots of the power laws [Eq. (2a)] yield f_c~0.10±0.01, 0.20±0.01, 0.08±0.01 and 0.18±0.01; and s'=0.99±0.02, 0.93±0.03, 1.06±0.03, and 0.85±0.03, respectively, for the NaTNO/PVDF composites investigated. The sequence of percolation threshold in the four kinds of NaTNO/PVDF composites, from high to low, corresponding to the conducting fillers, can be arranged as NaTNO-1C, NaTNO-2C, NaTNO-1, and NaTNO-2. Compared with the corresponding results reported in the polymer/conductive filler composites, [24, 33-38] the percolation thresholds of the NaTNO/PVDF composite are quite low due to a high aspect ratio and the unique physical properties of NaTNO employed [24].

The conductivities of two ceramics, NaTNO-1C and NaTNO-2C, increase with increasing temperature as shown in inset of Figure. 4(a); such behavior is an important feature for the semiconducting materials. The conductivity of the NaTNO-2C ceramic is larger than that of NaTNO-1C due to a higher Na content in the NaTNO-2C ceramic. In addition, the conductivities of the NaTNO-1 and NaTNO-2 powders without sintering treatment are relatively higher than those of the NaTNO-1C and NaTNO-2C composites. This is due to little volatilization of Na salt during sintering. Therefore, the descending order of conductivities of four NaTNO samples is arranged as NaTNO-2, NaTNO-1, NaTNO-2C, and NaTNO-1C. In comparison with the sequence of percolation threshold referred above, the results showed that the percolation threshold f_c of the NaTNO/PVDF composites increased as the conductivity of the filler decreased. It is obvious that the conductivity of NaTNO fillers [24, 30] plays an important role on the percolation threshold of the NaTNO/PVDF composites. The universality of the percolation theory suggests that the ε_{eff} should exhibit the same power-low dependence on the volume fraction as the conductivity below f_c, i.e., $s \approx s'$~1, but this is not always observed in practical continuum systems [9, 34]. Compared to the results of the KTNO/PVDF (K and Ti co-doped NiO) and LNO/PVDF composites, [28, 37] the percolation thresholds of the NaTNO/

PVDF composites were quite low due to lower grain size of the filler particles as well as nonspherical morphology of the fillers. Partial agglomeration of a large number of NaTNO-2C particles can be seen in the NaTNO-2C/PVDF composite as the NaTNO-2C particles possess a large surface energy resulting from grinding the NaTNO-2C ceramic into very small particles. Grinding caused surface modulation. Furthermore, the percolation threshold of the NaTNO-2C/PVDF composite is higher than that of the NaTNO-2/PVDF composite. Therefore, the mechanical property of the NaTNO-2C/PVDF composite could be poorer than that of the NaTNO-2/PVDF composite. It is noted that the dielectric loss of the percolation NaTNO/PVDF composite is as high as 0.18 at RT and low frequency, 1 kHz, as shown in figure 4(d). It was speculated that, in a well-dispersed PNC, interfaces between the nanoparticle and polymer phases created effective electron scattering and transport centers, thus reducing the percolation threshold. Moreover, well-dispersed ceramic particles should block degradation of particle cluster and thus increased the percolation threshold [21-25]. Like dielectric constant and conductivity, the dielectric loss of the composites increased rapidly with the approach of percolation threshold. The increased dielectric loss for the composites was due to the effect of the electrically semiconducting nature of NaTNO and eddy current loss due to the close proximity of the semiconducting fillers. Therefore, these types of composites might be used as high charge-storage capacitors of various shape and sizes due to their flexibility.

Figures 4 (c and d) showed the frequency dependent electrical conductivity (σ_{eff}) and dielectric loss tangent (tanδ) of the percolative PVDF/NaTNO composites. For $f_{\text{NaTNO}} < f_c$, the conductivity increased almost linearly with increasing frequency; whreas for $f_{\text{NaTNO}} > f_c$, the conductivity values were much higher than those samples with $f_{\text{NaTNO}} < f_c$, and weree almost independent of frequency in the low-frequency region. Furthermore, the log–log plots of frequency dependent conductivity yielded a straight line a typical characteristic of the percolative composites. According to the percolation theory, [33-38] as $f_{\text{NaTNO}} \rightarrow f_c$,

$$\sigma_{eff} \propto \omega^{u}, \varepsilon_{eff} \propto \omega^{u-1} \tag{3}$$

where $\omega = 2\pi\nu$ and u is a critical exponent. The data for all percolative NaTNO/PVDF composites yield $u \approx 0.84$, 0.92, 0.88, and 0.94. This result showed that the value of u *was* almost the same for percolative composites NaTNO-1/PVDF and NaTNO-2/PVDF (0.84 and 0.88); and also for the NaTNO-1C/PVDF and NaTNO-2C/PVDF composites (0.92 and 0.94). The conductivity data

for f_c=0.18 for NaTNO-2C/PVDF composite were fitted to Eq. (3) as shown in the inset of figure 4(c), with u=0.94±0.04 which was little larger than the universal value (u_{un}~0.73) [9]. The loss tangents in figure 4(d) underwent a sharp increase at high frequencies while maintaining a value below 0.18 at high frequencies.

The temperature dependent dielectric constant for the 0.10NaTNO-1+PVDF composite was shown in figure 5(a); at various fixed frequencies indicated an anomaly in the temperature range 250–330 K which was related to a freezing dipolar motion in the amorphous region. At ~425K, the observed anomaly in the real part of dielectric permittivity (ε') indicated the characteristic ferroelectric-paraelectric phase transition. The diffused dielectric anomaly obtained for the NaTNO-1/PVDF sample in the 250–350 K temperature range as well as the characteristic dispersion of the permittivity represented the signatures of the high-ε_r [31-32] properties of the ceramics used to produce NaTNO/PVDF composites. In the low temperature range, the described maxima of tanδ (Inset of figure 5(a)) increased and shifted towards higher temperatures with increasing frequency, whereas in the high temperature regime, the maxima decreased with increasing frequency. A cusp-like behavior in the frequency and temperature dependence of the $\varepsilon_{eff}(v, T)$ curve in the temperature range (T=250-303K) accompanied by absorption maxima shifting towards higher temperatures with increasing frequency, which was related to the freezing of dipolar motion in the amorphous region of the polymer. The value of ε_{eff} dropped gradually when the temperature further increased up to 408K above which the composite became flexible enough and the movements of the molecules increased. A similar phenomenon was also observed for the $BaTiO_3$/PVDF [39] and the CCTO/PVDF [38] composites systems. The leakage current also increased with increasing content of NaTNO in the composite due to the increased loss of hydrophobicity as well as reduced surface resistivity of the insulator. It was expected that the higher NaTNO composites would cause the insulator surface more wetted and higher leakage current would flow due to the lower surface resistivity. Effect of leakage current flow on the surface would cause dry bands to be formed at the thinnest conducting film, where the surface leakage current density was highest. The leakage current **J** (A/cm^2) as a function of applied electric field **E** (kV/cm) were shown in figure 5(b) for all the percolative composites (the maximum is still below 2×10^{-5} A/cm^2). Inset of figure 5(b) also presented the variation of the effective piezoelectric coefficient d_{33} (pC/N) in the neighborhood

of the percolation threshold [33-38]. The piezoelecric coefficient is given by the following power law

$$d_{33} \propto (f_c - f)^q \quad (4)$$

where q is a critical exponent which is about 1.46, calculated from inset of figure 5(b).

The dependence of the breakdown strength on the volume fraction of NaTNO nanofillers was shown in figure 6(a). The PVDF matrix employed showed the dielectric breakdown strength (E_b) of 250kV/mm (Figure 6(a)). With the introduction of NaTNO-2 nanofillers, E_b of the composites gradually decreased from pure PVDF matrix and with further addition of NaTNO, yet it was still ~180 kV/mm at the highest NaTNO nanofillers loading of 10 vol.%, as shown in figure 6(a). It is worth noting that very similar dependences of breakdown strengths on the content of dielectric fillers, i.e., enhanced E_b at low loading of fillers followed by marked decrease in E_b upon further addition of dielectric fillers were also observed earlier by different research groups number of researchers [39-41]. It is generally accepted that, in general, a small amount of fillers are in favor of tightly bonding the polymer chains to the fillers, which decreases the mobility of the polymer chains and also leads to smaller probability of charge transferring during electric breakdown [39-40]. When percolation occurs, the breakdown strength will be abruptly reduced, as the charge conduction along the percolative pathways can occur, facilitating the breakdown. As a result, the magnitude of the drop in the breakdown strength in this regime can be mitigated as compared to the PNC with unmodified *nps* [38]. In our present study, the onset of such a percolation pathway occurred between the volume fractions 8 and 18 vol% in the case of NaTNO. Figure 6(a) also displayed the tensile strength of NaTNO/PVDF hybrid nanocomposites films as a function of volume content. The tensile strength at room (300*K*) temperature increased first to a maximum, and afterwards decreased with increasing volume content [38, 41]. It was noticed that increase in filler content reduced the strength of composites with an average particle diameter of 80 nm. The composite strength decreased with increasing NaTNO content and it was lower than that of the polymer matrix; but better interfacial adhesion provided a higher composite strength. The *P-E* curves for the PVDF-based composites with different amounts of NaTNO fillers were shown in figure 6(b). The saturation polarization (P_s) increased consistently from ~7.6μC/cm^2 for pure PVDF to ~8.2μC/cm^2 for the composites with 10 vol. % of NaTNO-1, while very little increase in the remnant polarization (P_r) was observed. Further introduction of NaTNO nanofillers resulted in a dramatic decrease in P_s, which was also

accompanied by simultaneous increase in leakage current density from ~0.1μC/cm^2 to ~1μC/cm^2 as the content of nanofillers increased from 2% to 10 vol%. The PNC films of our present investigation were almost one order of magnitude thicker than those of the commercial dielectric polymer sheets (e.g., 3–5 μm), resulting in more defects or weak points and thus leading to decreased breakdown strength. A further reduction of the film thickness promises higher breakdown strength [42] and hence further enhancement of ferroelectric properties in these NaTNO based polymer nanocomposites.

4. Conclusion

In conclusion, significantly enhanced dielectric constants as well as ferroelectric polarization along with improved breakdown strength were achieved in PVDF-based composites filled with new NaTNO semiconducting nanoparticles. The percolation threshold f_c in the NaTNO/PVDF composites decreased with decrease of particle size and DC conductivity of the semiconducting fillers. The NaTNO/PVDF composites exhibited a relatively high dielectric constants and conductivities near the low percolation threshold. The results of ferroelectric and dielectric measurements indicated percolation threshold f_c~ 0.10 as the optimum one which provided the highest dielectric and breakdown strength of the NaTNO-1/PVDF nanocomposites. The low volume fraction (f_c) of NaTNO kept optimum flexibility of the composite as well as sustained the ferroelectric behavior of the PVDF polymer in the composite almost unaltered up to the percolation limit suitable for technological applications. Therefore, these kinds of semiconductive and low percolative NaTNO/PVDF nanocomposites with a low leakage current and high dielectric constant with low loss might be considered as potential candidates to fabricate high charge-storage capacitors with various shapes due to their flexibility and mechanical stability.

Acknowledgements: Authors are grateful to the IACS for providing experimental facilities to complete the work. BKC also acknowledges the AvH Foundation for providing Impedance analyzer as gift. DB is grateful to Department of Science and Technology (DST), Government of India, for providing major facility to carry out this work.

TABLE I. Physical properties of NaTNO fillers (bulk and nano) in NaTNO/PVDF composites

Sample	Stoichiometry mixed with PVDF	Particle Size (μm/nm)	Percolation Threshold (f_c)	AC Conductivity (σ_{eff})(S/m) Percolative	ε_{eff}	Electrical property σ_{DC} (S/m)
NaTNO-1C	$Na_{0.05}Ti_{0.02}Ni_{0.9}O$	0.75μm	0.20	2.18×10^{-6}	650	semiconductor
NaTNO-1	$Na_{0.05}Ti_{0.02}Ni_{0.9}O$	90nm	0.10	1.45×10^{-6}	710	1.5×10^{-4} semiconductor
NaTNO-2C	$Na_{0.15}Ti_{0.02}Ni_{0.8}O$	0.50μm	0.18	2.1×10^{-6}	630	2.7×10^{-4} semiconductor
NaTNO-2	$Na_{0.15}Ti_{0.02}Ni_{0.8}O$	80nm	0.08	1.92×10^{-6}	640	3.2×10^{-4} semiconductor 4.1×10^{-4}

*NaTNO-1 and NaTNO-2 are nano-structure particles and NaTNO-1C and NaTNO-2C are corresponding ceramic micro-structure particles

References

[1] L. Zhang, and Z.-Y. Cheng, , J. Adv. Dielectrics. 1, 389 (2011).

[2] Z. M. Dang, J. K. Yuan, J. W. Zha, T. Zhou, S. T. Li, and G. H. Hu, Prog. Mater. Sci. 57, 660 (2012).

[3] C. W. Nan, Y. Shen and J. Ma, Annu. Rev. Mater. Res. 40, 131(2010).

[4] Goel M. *Ceram. Int.* 2004; *30*, 1147.

[5] Z. M. Dang, T. Zhou, S. H. Yao, J. K. Yuan, J. W. Zha, H. T. Song, J. Y. Li, Q. Chen, W. T. Yang and J. B. Bai, Adv. Mater. 21, 2077 (2009).

[6] L. Zhang, P.X. Wu, Y.T. Li, J. Z.-Y Cheng, and J.C. Brewer, Composites B, 56, 284 (2014).

[7] Sychov M.M., Zakharova N.V., Mjakin S.V. Ceramics International, 39, 6821 (2013)

[8] Bai Y, Cheng ZY, Bharti V, Xu HS, and Zhang QM. Appl Phys Lett 2000; 76, 3804.

[9] Nan CW. Prog Mater Sci 1993; 37, 1.

[10] M. Panda, V. Srinivas, and A. K. Thakur, Appl. Phys. Lett. 92, 132905 (2008).

[11] L. Zhang, P. Bass, and Z.-Y Cheng, Appl. Phys. Lett. 105, 042905 (2014).

[12] Yao SH, Dang ZM, Jiang MJ, Xu HP and Bai J. Appl Phys Lett 2007; 91, 212901.

[13] Wang L and Dang ZM. Appl Phys Lett 2005; 87, 042903

[14] Dang ZM, Wang L, Yin Y, Zhang Q and Lei QQ. Adv Mater 2007; 19, 852

[15] Huang C and Zhang QM. Appl Phys Lett 2003; 82, 20

[16] He S, Wang GS, Lu C, Luo X, Wen B, Guo L and Cao MS. J Mater Chem A 2013; 1, 4685.

[17] Liu XG, Geng DY, Meng H, Shang PJ and Zhang ZD. Appl Phys Lett 2008; 92, 173117.

[18] He S, Wang GS, Lu C, Luo X, Wen B, Guo L and Cao MS. Chem Plus Chem 2013; 78, 250

[19] Li J, Seok S. Il, Chu B, Dogan F, Zhang Q and Wang Q. Adv Mater 2009; 21, 217.

[20] Zhang SH, Zhang NY, Huang C, Ren KL and Zhang QM. Adv Mater 2005; 17, 1897.

[21] Dang ZM, Zhou T, Yao SH, Yuan JK, Zha JW, Song HT, Li JY, Chen Q, Yang WT and Bai J. Adv Mater 2009; 21, 1

[22] Wu JB, Nan CW, Lin YH and Deng Y. Phys. Rev. Lett. 2002; 89, 217601

[23] Lin Y, Jiang L, Zhao R and Nan C W 2002 *Phys. Rev.* B **72** 014103

[24] Jana PK, Sarkar S, Sakata H, Watanabe T and Chaudhuri BK. J Phys D: Appl Phys 2008; 41, 065403

[25] Dargaville TR, Celina M, Chaplya PM. J. Polymer Sci. Part B: Polymer Phys. 2005; *43*, 1310.

[26] Bhadra D, Masud MG, Sarkar S, Sannigrahi J, De SK and Chaudhuri BK. J Polm Sci Part b: Polym Phys 2012; 50, 572.
[27] Chen M, Tao T, Zhang L, Gao W and Li C. Chem Comm 2013; 49, 1612.
[28] Bhadra D, Biswas A, Sarkar S, Tseng KF, Yang HD and Chaudhuri BK. J Appl Phys 2010; 107, 124115.

[29] Bhadra D, Masud MG, De SK and Chaudhuri BK. J Phys D: Appl Phys 2012; 45, 485002.

[30] Jana PK, Sarkar S, Karmakar S and Chaudhuri BK. J Appl Phys 2007; 102, 084105
[31] H. P. Xu, H. Q. Xie, D. D. Yang, Y. H. Wu, and J. R. Wang, J. Appl. Polym. Sci. 122, 3466 (2011).
[32] L. Zhang, X. B. Shan, P. X. Wu and Z.-Y. Cheng, J. Appl. Phys. A 107, 597 (2012).
[33] Chiteme C and Mclachlan DS. Physica B 2000; 279, 69.

[34] Efros AL and Shklovskii BI. Phys Status Solidi B 1976; 76, 475.

[35] Bergman DJ and Imry Y. Phys Rev Lett 1977; 39, 1222.

[36] Pecharroman C, Fatima EB and Moya JS. Adv Mater 2000; 12, 294.

[37] Dang ZM, Nan CW, Xie D, Zhang YH and Tjong SC. Appl Phys Lett 2004; 85, 97.
[38] Arbatti M, Shan X and Cheng ZY. Adv Mater 2007; 19, 1369.

[39] Dang ZM, Yuan JK, Yao SH, Liao RJ. Adv Mater 2013; 25, 6334.
[40] Hergeth WD, Steinau UJ, Bittrich HJ, Simon G, Schmutzler K. Polymer 1989; 30, 254.

[41] Jiang L, Zhang J, Wolcott MP. Polymer 2007; 48, 7632.
[42] Dang ZM, Yuan JK, Zha JW, Zhou T, Li ST, Hu GH. Progress in Materials Science 2012; 57, 660.

Figure captions

Figure 1. (Color online). (a) FESEM image of NaTNO-1 and (b) NaTNO-2 nanoparticles. Inset (a (left corner) and b (right corner)) shows the grain morphologies of NaTNO-1C and 2C ceramic powders respectively. Inset (a (right corner) and b (left below)) shows the TEM image of as-prepared NaTNO-1 and 2 nanoparticles. (c) SEM micrograph showing the polished surface and (d) fractured surface of NaTNO-1/PVDF nanocomposite at the percolation threshold. (e) SEM micrograph showing the polished surface and (d) fractured cross-section of NaTNO-1C/PVDF composite at the percolation threshold.

Figure 2. (Color online) XRD patterns of (a) NaTNO-1C and NaTNO-1 nanoparticles (b) their composites with PVDF polymer (c) NaTNO-2C and NaTNO-2 nanoparticles (d) their composites with PVDF polymer.

Figure 3. (Color online) Dependence of (a) effective permittivity (ε_{eff}) of the NaTNO/PVDF composites on the NaTNO volume fraction, f_{NaTNO} at RT. (b) Fitting of the critical exponent (s) derived from Eq. 1. (c) shows tanδ Vs f_{NaTNO} showing percolative behavior. (d) Frequency dispersion of real part of dielectric permittivity and AC conductivity curves of NaTNO-1C and 2C (inset shows the microstructures of typical NaTNO-1(left) and NaTNO-2(right) ceramics) (e) ε_{eff} of the percolative NaTNO/PVDF composites as a function of frequency at RT.

Figure 4. (Color online). Dependence of (a) effective conductivity (σ_{eff}) of the NaTNO/PVDF composites on the NaTNO volume fraction, f_{NaTNO} at RT. Inset of (a) shows temperature dependence of the conductivity of semiconducting NaTNO ceramics. (b) Fitting of the critical exponent (s′ and t) derived from Eq. 2. (c) σ_{eff} and (d) loss tangent (tanδ) of the percolative NaTNO/PVDF percolative composites as a function of frequency at RT. Inset of (c) shows the linear fitting parameters (u) obtained from Eq. 3 in case of NaTNO-2C/PVDF composite.

Figure 5. (Color online) Temperature variation in ε_{eff} of the $f_{NaTNO\text{-}1}$=0.10 nanocomposite with different fixed frequencies. (b) Leakage current densities (***J***) as a function of applied electric field (***E*** in kV/cm) for different NaTNO percolative concentrations. Upper inset of (a) shows the magnifying part of peak shifting and lower shows tanδ vs T plot with increasing frequency. Inset of (b) shows piezoelectric coefficient of NaTNO-1/PVDF with varying concentrations.

Figure 6. (Color online) (a) Variations of the tensile strength and breakdown voltage (E_b) of NaTNO/PVDF nanocomposites for different volume fractions of NaTNO 1 & 2 nanofillers. (b) *P–E* hysteresis loops for NaTNO/PVDF composites with different volume fractions of NaTNO at RT.

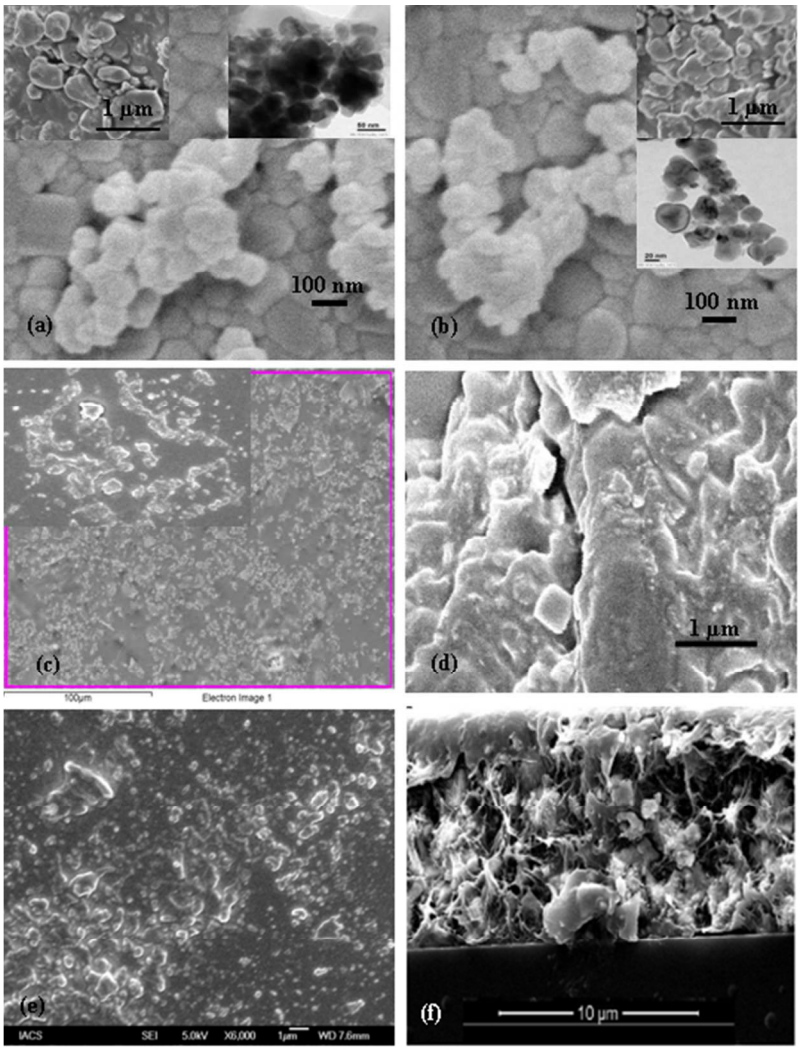

FIG. 1

142x214mm (96 x 96 DPI)

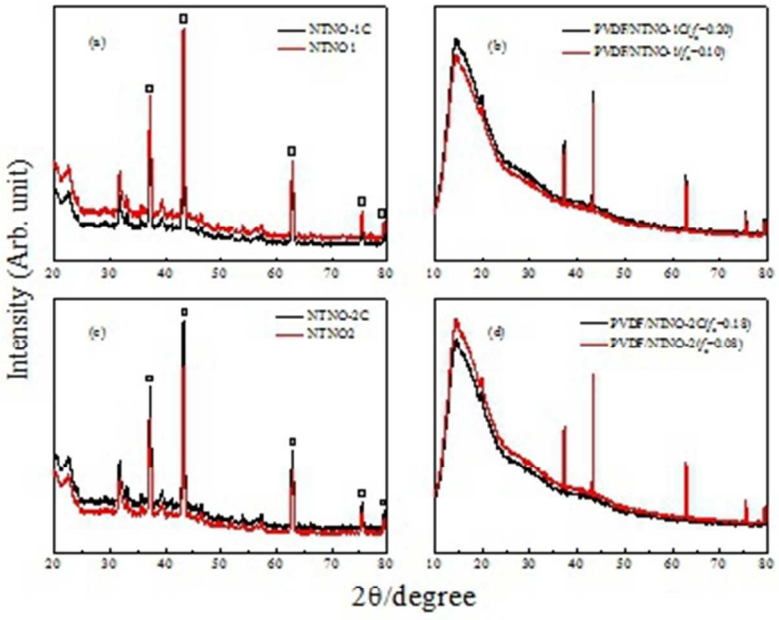

FIG. 2

106x95mm (96 x 96 DPI)

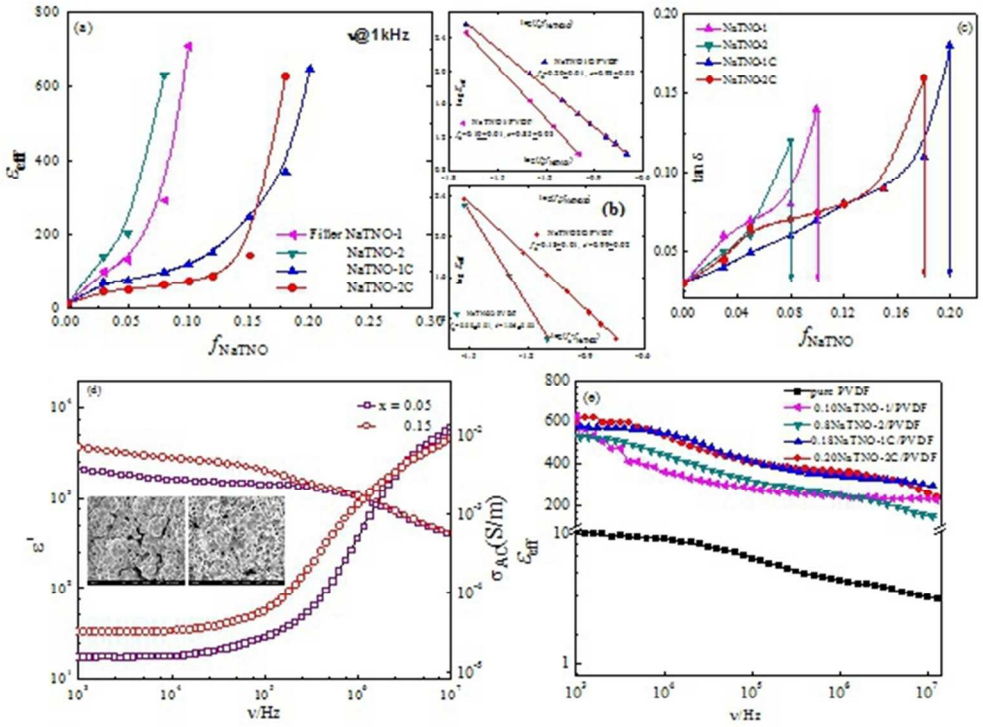

FIG. 3

157x130mm (96 x 96 DPI)

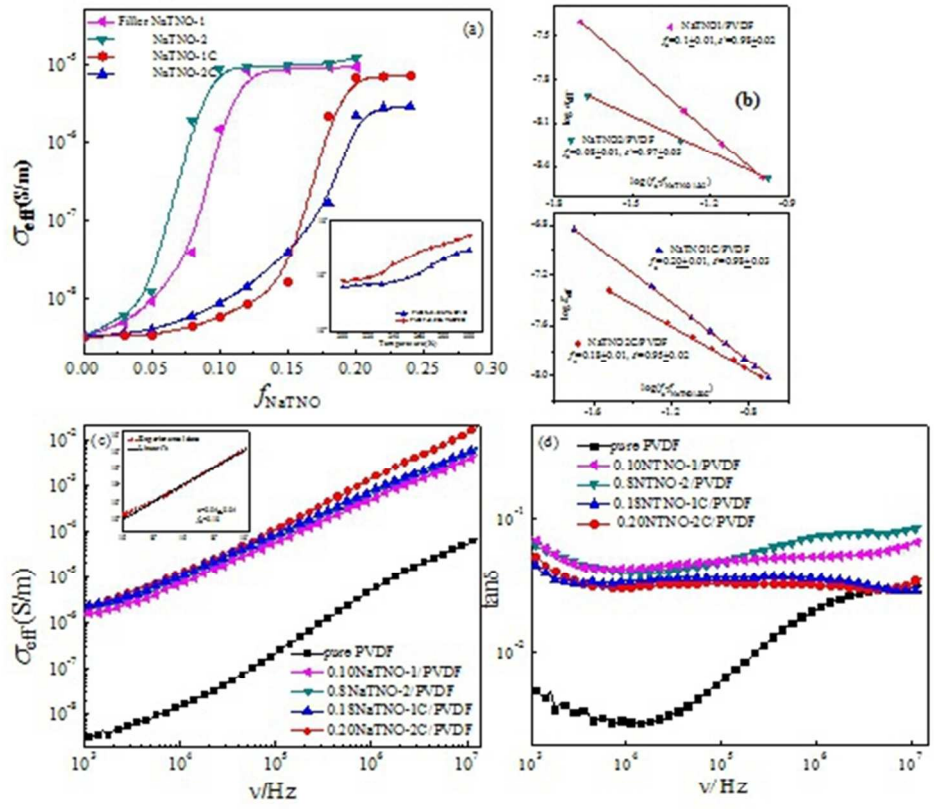

FIG. 4

144x136mm (96 x 96 DPI)

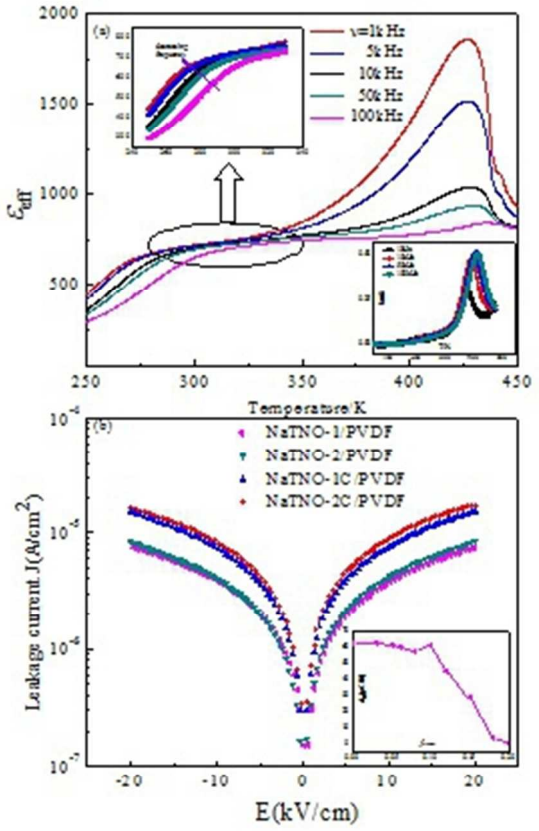

Fig. 5

75x128mm (96 x 96 DPI)

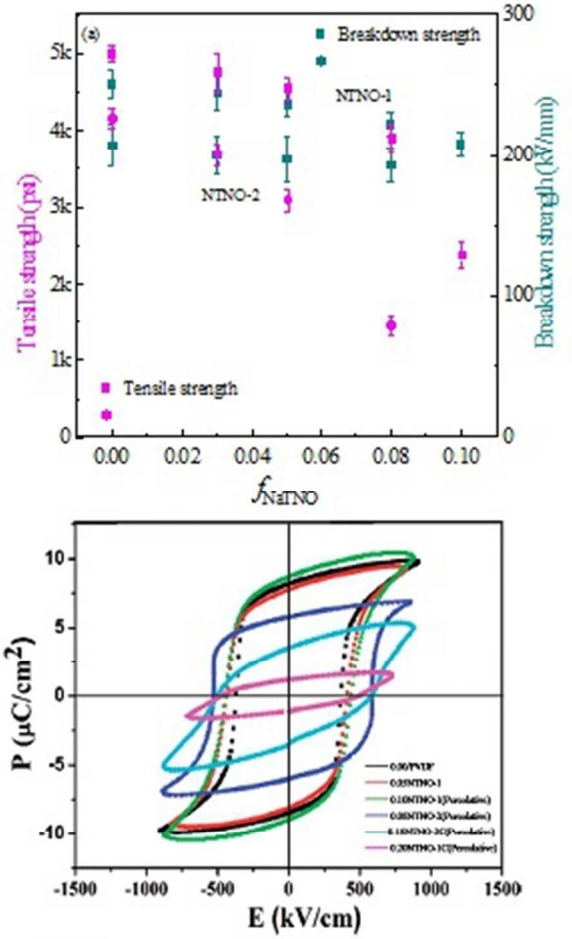

FIG. 6

76x135mm (96 x 96 DPI)